September 2002

*BABAR*-PUB-02/06
SLAC-PUB-9261
hep-ex/0209013

# A Measurement of the $B^0 \to J/\psi\pi^+\pi^-$ Branching Fraction

B. Aubert,[1] D. Boutigny,[1] J.-M. Gaillard,[1] A. Hicheur,[1] Y. Karyotakis,[1] J. P. Lees,[1] P. Robbe,[1] V. Tisserand,[1] A. Zghiche,[1] A. Palano,[2] A. Pompili,[2] J. C. Chen,[3] N. D. Qi,[3] G. Rong,[3] P. Wang,[3] Y. S. Zhu,[3] G. Eigen,[4] I. Ofte,[4] B. Stugu,[4] G. S. Abrams,[5] A. W. Borgland,[5] A. B. Breon,[5] D. N. Brown,[5] J. Button-Shafer,[5] R. N. Cahn,[5] E. Charles,[5] M. S. Gill,[5] A. V. Gritsan,[5] Y. Groysman,[5] R. G. Jacobsen,[5] R. W. Kadel,[5] J. Kadyk,[5] L. T. Kerth,[5] Yu. G. Kolomensky,[5] J. F. Kral,[5] C. LeClerc,[5] M. E. Levi,[5] G. Lynch,[5] L. M. Mir,[5] P. J. Oddone,[5] T. J. Orimoto,[5] M. Pripstein,[5] N. A. Roe,[5] A. Romosan,[5] M. T. Ronan,[5] V. G. Shelkov,[5] A. V. Telnov,[5] W. A. Wenzel,[5] T. J. Harrison,[6] C. M. Hawkes,[6] D. J. Knowles,[6] S. W. O'Neale,[6] R. C. Penny,[6] A. T. Watson,[6] N. K. Watson,[6] T. Deppermann,[7] K. Goetzen,[7] H. Koch,[7] B. Lewandowski,[7] K. Peters,[7] H. Schmuecker,[7] M. Steinke,[7] N. R. Barlow,[8] W. Bhimji,[8] J. T. Boyd,[8] N. Chevalier,[8] P. J. Clark,[8] W. N. Cottingham,[8] C. Mackay,[8] F. F. Wilson,[8] K. Abe,[9] C. Hearty,[9] T. S. Mattison,[9] J. A. McKenna,[9] D. Thiessen,[9] S. Jolly,[10] A. K. McKemey,[10] V. E. Blinov,[11] A. D. Bukin,[11] A. R. Buzykaev,[11] V. B. Golubev,[11] V. N. Ivanchenko,[11] A. A. Korol,[11] E. A. Kravchenko,[11] A. P. Onuchin,[11] S. I. Serednyakov,[11] Yu. I. Skovpen,[11] A. N. Yushkov,[11] D. Best,[12] M. Chao,[12] D. Kirkby,[12] A. J. Lankford,[12] M. Mandelkern,[12] S. McMahon,[12] D. P. Stoker,[12] K. Arisaka,[13] C. Buchanan,[13] S. Chun,[13] D. B. MacFarlane,[14] S. Prell,[14] Sh. Rahatlou,[14] G. Raven,[14] V. Sharma,[14] J. W. Berryhill,[15] C. Campagnari,[15] B. Dahmes,[15] P. A. Hart,[15] N. Kuznetsova,[15] S. L. Levy,[15] O. Long,[15] A. Lu,[15] M. A. Mazur,[15] J. D. Richman,[15] W. Verkerke,[15] J. Beringer,[16] A. M. Eisner,[16] M. Grothe,[16] C. A. Heusch,[16] W. S. Lockman,[16] T. Pulliam,[16] T. Schalk,[16] R. E. Schmitz,[16] B. A. Schumm,[16] A. Seiden,[16] M. Turri,[16] W. Walkowiak,[16] D. C. Williams,[16] M. G. Wilson,[16] E. Chen,[17] G. P. Dubois-Felsmann,[17] A. Dvoretskii,[17] D. G. Hitlin,[17] F. C. Porter,[17] A. Ryd,[17] A. Samuel,[17] S. Yang,[17] S. Jayatilleke,[18] G. Mancinelli,[18] B. T. Meadows,[18] M. D. Sokoloff,[18] T. Barillari,[19] P. Bloom,[19] W. T. Ford,[19] U. Nauenberg,[19] A. Olivas,[19] P. Rankin,[19] J. Roy,[19] J. G. Smith,[19] W. C. van Hoek,[19] L. Zhang,[19] J. Blouw,[20] J. L. Harton,[20] M. Krishnamurthy,[20] A. Soffer,[20] W. H. Toki,[20] R. J. Wilson,[20] J. Zhang,[20] D. Altenburg,[21] T. Brandt,[21] J. Brose,[21] T. Colberg,[21] M. Dickopp,[21] R. S. Dubitzky,[21] A. Hauke,[21] E. Maly,[21] R. Müller-Pfefferkorn,[21] S. Otto,[21] K. R. Schubert,[21] R. Schwierz,[21] B. Spaan,[21] L. Wilden,[21] D. Bernard,[22] G. R. Bonneaud,[22] F. Brochard,[22] J. Cohen-Tanugi,[22] S. Ferrag,[22] S. T'Jampens,[22] Ch. Thiebaux,[22] G. Vasileiadis,[22] M. Verderi,[22] A. Anjomshoaa,[23] R. Bernet,[23] A. Khan,[23] D. Lavin,[23] F. Muheim,[23] S. Playfer,[23] J. E. Swain,[23] J. Tinslay,[23] M. Falbo,[24] C. Borean,[25] C. Bozzi,[25] L. Piemontese,[25] A. Sarti,[25] E. Treadwell,[26] F. Anulli,[27,*] R. Baldini-Ferroli,[27] A. Calcaterra,[27] R. de Sangro,[27] D. Falciai,[27] G. Finocchiaro,[27] P. Patteri,[27] I. M. Peruzzi,[27,*] M. Piccolo,[27] A. Zallo,[27] S. Bagnasco,[28] A. Buzzo,[28] R. Contri,[28] G. Crosetti,[28] M. Lo Vetere,[28] M. Macri,[28] M. R. Monge,[28] S. Passaggio,[28] F. C. Pastore,[28] C. Patrignani,[28] E. Robutti,[28] A. Santroni,[28] S. Tosi,[28] M. Morii,[29] R. Bartoldus,[30] G. J. Grenier,[30] U. Mallik,[30] J. Cochran,[31] H. B. Crawley,[31] J. Lamsa,[31] W. T. Meyer,[31] E. I. Rosenberg,[31] J. Yi,[31] M. Davier,[32] G. Grosdidier,[32] A. Höcker,[32] H. M. Lacker,[32] S. Laplace,[32] F. Le Diberder,[32] V. Lepeltier,[32] A. M. Lutz,[32] T. C. Petersen,[32] S. Plaszczynski,[32] M. H. Schune,[32] L. Tantot,[32] S. Trincaz-Duvoid,[32] G. Wormser,[32] R. M. Bionta,[33] V. Brigljević,[33] D. J. Lange,[33] M. Mugge,[33] K. van Bibber,[33] D. M. Wright,[33] A. J. Bevan,[34] J. R. Fry,[34] E. Gabathuler,[34] R. Gamet,[34] M. George,[34] M. Kay,[34] D. J. Payne,[34] R. J. Sloane,[34] C. Touramanis,[34] M. L. Aspinwall,[35] D. A. Bowerman,[35] P. D. Dauncey,[35] U. Egede,[35] I. Eschrich,[35] G. W. Morton,[35] J. A. Nash,[35] P. Sanders,[35] D. Smith,[35] G. P. Taylor,[35] J. J. Back,[36] G. Bellodi,[36] P. Dixon,[36] P. F. Harrison,[36] R. J. L. Potter,[36] H. W. Shorthouse,[36] P. Strother,[36] P. B. Vidal,[36] G. Cowan,[37] H. U. Flaecher,[37] S. George,[37] M. G. Green,[37] A. Kurup,[37] C. E. Marker,[37] T. R. McMahon,[37] S. Ricciardi,[37] F. Salvatore,[37] G. Vaitsas,[37] M. A. Winter,[37] D. Brown,[38] C. L. Davis,[38] J. Allison,[39] R. J. Barlow,[39] A. C. Forti,[39] F. Jackson,[39] G. D. Lafferty,[39] N. Savvas,[39] J. H. Weatherall,[39] J. C. Williams,[39] A. Farbin,[40] A. Jawahery,[40] V. Lillard,[40] D. A. Roberts,[40] J. R. Schieck,[40] G. Blaylock,[41] C. Dallapiccola,[41] K. T. Flood,[41] S. S. Hertzbach,[41] R. Kofler,[41] V. B. Koptchev,[41] T. B. Moore,[41] H. Staengle,[41] S. Willocq,[41] B. Brau,[42] R. Cowan,[42] G. Sciolla,[42] F. Taylor,[42] R. K. Yamamoto,[42] M. Milek,[43] P. M. Patel,[43] F. Palombo,[44] J. M. Bauer,[45] L. Cremaldi,[45] V. Eschenburg,[45] R. Kroeger,[45] J. Reidy,[45]

Work supported in part by the Department of Energy contract DE-AC03-76SF00515.

Stanford Linear Accelerator Center, Stanford University, Stanford, CA, 94309

D. A. Sanders,[45] D. J. Summers,[45] C. Hast,[46] P. Taras,[46] H. Nicholson,[47] C. Cartaro,[48] N. Cavallo,[48] G. De Nardo,[48] F. Fabozzi,[48] C. Gatto,[48] L. Lista,[48] P. Paolucci,[48] D. Piccolo,[48] C. Sciacca,[48] J. M. LoSecco,[49] J. R. G. Alsmiller,[50] T. A. Gabriel,[50] J. Brau,[51] R. Frey,[51] M. Iwasaki,[51] C. T. Potter,[51] N. B. Sinev,[51] D. Strom,[51] E. Torrence,[51] F. Colecchia,[52] A. Dorigo,[52] F. Galeazzi,[52] M. Margoni,[52] M. Morandin,[52] M. Posocco,[52] M. Rotondo,[52] F. Simonetto,[52] R. Stroili,[52] C. Voci,[52] M. Benayoun,[53] H. Briand,[53] J. Chauveau,[53] P. David,[53] Ch. de la Vaissière,[53] L. Del Buono,[53] O. Hamon,[53] Ph. Leruste,[53] J. Ocariz,[53] M. Pivk,[53] L. Roos,[53] J. Stark,[53] P. F. Manfredi,[54] V. Re,[54] V. Speziali,[54] L. Gladney,[55] Q. H. Guo,[55] J. Panetta,[55] C. Angelini,[56] G. Batignani,[56] S. Bettarini,[56] M. Bondioli,[56] F. Bucci,[56] G. Calderini,[56] E. Campagna,[56] M. Carpinelli,[56] F. Forti,[56] M. A. Giorgi,[56] A. Lusiani,[56] G. Marchiori,[56] F. Martinez-Vidal,[56] M. Morganti,[56] N. Neri,[56] E. Paoloni,[56] M. Rama,[56] G. Rizzo,[56] F. Sandrelli,[56] G. Triggiani,[56] J. Walsh,[56] M. Haire,[57] D. Judd,[57] K. Paick,[57] L. Turnbull,[57] D. E. Wagoner,[57] J. Albert,[58] P. Elmer,[58] C. Lu,[58] V. Miftakov,[58] J. Olsen,[58] S. F. Schaffner,[58] A. J. S. Smith,[58] A. Tumanov,[58] E. W. Varnes,[58] F. Bellini,[59] G. Cavoto,[58,59] D. del Re,[14,59] R. Faccini,[14,59] F. Ferrarotto,[59] F. Ferroni,[59] E. Leonardi,[59] M. A. Mazzoni,[59] S. Morganti,[59] G. Piredda,[59] F. Safai Tehrani,[59] M. Serra,[59] C. Voena,[59] S. Christ,[60] G. Wagner,[60] R. Waldi,[60] T. Adye,[61] N. De Groot,[61] B. Franek,[61] N. I. Geddes,[61] G. P. Gopal,[61] S. M. Xella,[61] R. Aleksan,[62] S. Emery,[62] A. Gaidot,[62] P.-F. Giraud,[62] G. Hamel de Monchenault,[62] W. Kozanecki,[62] M. Langer,[62] G. W. London,[62] B. Mayer,[62] G. Schott,[62] B. Serfass,[62] G. Vasseur,[62] Ch. Yeche,[62] M. Zito,[62] M. V. Purohit,[63] A. W. Weidemann,[63] F. X. Yumiceva,[63] I. Adam,[64] D. Aston,[64] N. Berger,[64] A. M. Boyarski,[64] M. R. Convery,[64] D. P. Coupal,[64] D. Dong,[64] J. Dorfan,[64] W. Dunwoodie,[64] R. C. Field,[64] T. Glanzman,[64] S. J. Gowdy,[64] E. Grauges,[64] T. Haas,[64] T. Hadig,[64] V. Halyo,[64] T. Himel,[64] T. Hryn'ova,[64] M. E. Huffer,[64] W. R. Innes,[64] C. P. Jessop,[64] M. H. Kelsey,[64] P. Kim,[64] M. L. Kocian,[64] U. Langenegger,[64] D. W. G. S. Leith,[64] S. Luitz,[64] V. Luth,[64] H. L. Lynch,[64] H. Marsiske,[64] S. Menke,[64] R. Messner,[64] D. R. Muller,[64] C. P. O'Grady,[64] V. E. Ozcan,[64] A. Perazzo,[64] M. Perl,[64] S. Petrak,[64] B. N. Ratcliff,[64] S. H. Robertson,[64] A. Roodman,[64] A. A. Salnikov,[64] T. Schietinger,[64] R. H. Schindler,[64] J. Schwiening,[64] G. Simi,[64] A. Snyder,[64] A. Soha,[64] S. M. Spanier,[64] J. Stelzer,[64] D. Su,[64] M. K. Sullivan,[64] H. A. Tanaka,[64] J. Va'vra,[64] S. R. Wagner,[64] M. Weaver,[64] A. J. R. Weinstein,[64] W. J. Wisniewski,[64] D. H. Wright,[64] C. C. Young,[64] P. R. Burchat,[65] C. H. Cheng,[65] T. I. Meyer,[65] C. Roat,[65] R. Henderson,[66] W. Bugg,[67] H. Cohn,[67] J. M. Izen,[68] I. Kitayama,[68] X. C. Lou,[68] F. Bianchi,[69] M. Bona,[69] D. Gamba,[69] L. Bosisio,[70] G. Della Ricca,[70] S. Dittongo,[70] L. Lanceri,[70] P. Poropat,[70] L. Vitale,[70] G. Vuagnin,[70] R. S. Panvini,[71] S. W. Banerjee,[72] C. M. Brown,[72] D. Fortin,[72] P. D. Jackson,[72] R. Kowalewski,[72] J. M. Roney,[72] H. R. Band,[73] S. Dasu,[73] M. Datta,[73] A. M. Eichenbaum,[73] H. Hu,[73] J. R. Johnson,[73] R. Liu,[73] F. Di Lodovico,[73] A. Mohapatra,[73] Y. Pan,[73] R. Prepost,[73] I. J. Scott,[73] S. J. Sekula,[73] J. H. von Wimmersperg-Toeller,[73] J. Wu,[73] S. L. Wu,[73] Z. Yu,[73] and H. Neal[74]

(The *BABAR* Collaboration)

[1]*Laboratoire de Physique des Particules, F-74941 Annecy-le-Vieux, France*
[2]*Università di Bari, Dipartimento di Fisica and INFN, I-70126 Bari, Italy*
[3]*Institute of High Energy Physics, Beijing 100039, China*
[4]*University of Bergen, Inst. of Physics, N-5007 Bergen, Norway*
[5]*Lawrence Berkeley National Laboratory and University of California, Berkeley, CA 94720, USA*
[6]*University of Birmingham, Birmingham, B15 2TT, United Kingdom*
[7]*Ruhr Universität Bochum, Institut für Experimentalphysik 1, D-44780 Bochum, Germany*
[8]*University of Bristol, Bristol BS8 1TL, United Kingdom*
[9]*University of British Columbia, Vancouver, BC, Canada V6T 1Z1*
[10]*Brunel University, Uxbridge, Middlesex UB8 3PH, United Kingdom*
[11]*Budker Institute of Nuclear Physics, Novosibirsk 630090, Russia*
[12]*University of California at Irvine, Irvine, CA 92697, USA*
[13]*University of California at Los Angeles, Los Angeles, CA 90024, USA*
[14]*University of California at San Diego, La Jolla, CA 92093, USA*
[15]*University of California at Santa Barbara, Santa Barbara, CA 93106, USA*
[16]*University of California at Santa Cruz, Institute for Particle Physics, Santa Cruz, CA 95064, USA*
[17]*California Institute of Technology, Pasadena, CA 91125, USA*
[18]*University of Cincinnati, Cincinnati, OH 45221, USA*
[19]*University of Colorado, Boulder, CO 80309, USA*
[20]*Colorado State University, Fort Collins, CO 80523, USA*
[21]*Technische Universität Dresden, Institut für Kern- und Teilchenphysik, D-01062 Dresden, Germany*
[22]*Ecole Polytechnique, LLR, F-91128 Palaiseau, France*
[23]*University of Edinburgh, Edinburgh EH9 3JZ, United Kingdom*
[24]*Elon University, Elon University, NC 27244-2010, USA*

[25]Università di Ferrara, Dipartimento di Fisica and INFN, I-44100 Ferrara, Italy
[26]Florida A&M University, Tallahassee, FL 32307, USA
[27]Laboratori Nazionali di Frascati dell'INFN, I-00044 Frascati, Italy
[28]Università di Genova, Dipartimento di Fisica and INFN, I-16146 Genova, Italy
[29]Harvard University, Cambridge, MA 02138, USA
[30]University of Iowa, Iowa City, IA 52242, USA
[31]Iowa State University, Ames, IA 50011-3160, USA
[32]Laboratoire de l'Accélérateur Linéaire, F-91898 Orsay, France
[33]Lawrence Livermore National Laboratory, Livermore, CA 94550, USA
[34]University of Liverpool, Liverpool L69 3BX, United Kingdom
[35]University of London, Imperial College, London, SW7 2BW, United Kingdom
[36]Queen Mary, University of London, E1 4NS, United Kingdom
[37]University of London, Royal Holloway and Bedford New College, Egham, Surrey TW20 0EX, United Kingdom
[38]University of Louisville, Louisville, KY 40292, USA
[39]University of Manchester, Manchester M13 9PL, United Kingdom
[40]University of Maryland, College Park, MD 20742, USA
[41]University of Massachusetts, Amherst, MA 01003, USA
[42]Massachusetts Institute of Technology, Laboratory for Nuclear Science, Cambridge, MA 02139, USA
[43]McGill University, Montréal, QC, Canada H3A 2T8
[44]Università di Milano, Dipartimento di Fisica and INFN, I-20133 Milano, Italy
[45]University of Mississippi, University, MS 38677, USA
[46]Université de Montréal, Laboratoire René J. A. Lévesque, Montréal, QC, Canada H3C 3J7
[47]Mount Holyoke College, South Hadley, MA 01075, USA
[48]Università di Napoli Federico II, Dipartimento di Scienze Fisiche and INFN, I-80126, Napoli, Italy
[49]University of Notre Dame, Notre Dame, IN 46556, USA
[50]Oak Ridge National Laboratory, Oak Ridge, TN 37831, USA
[51]University of Oregon, Eugene, OR 97403, USA
[52]Università di Padova, Dipartimento di Fisica and INFN, I-35131 Padova, Italy
[53]Universités Paris VI et VII, Lab de Physique Nucléaire H. E., F-75252 Paris, France
[54]Università di Pavia, Dipartimento di Elettronica and INFN, I-27100 Pavia, Italy
[55]University of Pennsylvania, Philadelphia, PA 19104, USA
[56]Università di Pisa, Scuola Normale Superiore and INFN, I-56010 Pisa, Italy
[57]Prairie View A&M University, Prairie View, TX 77446, USA
[58]Princeton University, Princeton, NJ 08544, USA
[59]Università di Roma La Sapienza, Dipartimento di Fisica and INFN, I-00185 Roma, Italy
[60]Universität Rostock, D-18051 Rostock, Germany
[61]Rutherford Appleton Laboratory, Chilton, Didcot, Oxon, OX11 0QX, United Kingdom
[62]DAPNIA, Commissariat à l'Energie Atomique/Saclay, F-91191 Gif-sur-Yvette, France
[63]University of South Carolina, Columbia, SC 29208, USA
[64]Stanford Linear Accelerator Center, Stanford, CA 94309, USA
[65]Stanford University, Stanford, CA 94305-4060, USA
[66]TRIUMF, Vancouver, BC, Canada V6T 2A3
[67]University of Tennessee, Knoxville, TN 37996, USA
[68]University of Texas at Dallas, Richardson, TX 75083, USA
[69]Università di Torino, Dipartimento di Fisica Sperimentale and INFN, I-10125 Torino, Italy
[70]Università di Trieste, Dipartimento di Fisica and INFN, I-34127 Trieste, Italy
[71]Vanderbilt University, Nashville, TN 37235, USA
[72]University of Victoria, Victoria, BC, Canada V8W 3P6
[73]University of Wisconsin, Madison, WI 53706, USA
[74]Yale University, New Haven, CT 06511, USA

(Dated: September 7, 2002)

We present a measurement of the branching fraction for the decay of the neutral $B$ meson into the final state $J/\psi\,\pi^+\pi^-$. The data set contains approximately 56 million $B\overline{B}$ pairs produced at the $\Upsilon(4S)$ resonance and recorded with the *BABAR* detector at the PEP-II asymmetric-energy $e^+e^-$ storage ring. The result of this analysis is $\mathcal{B}(B^0 \to J/\psi\,\pi^+\pi^-) = (4.6 \pm 0.7 \pm 0.6)\times 10^{-5}$, where the first error is statistical and the second is systematic. In addition we measure $\mathcal{B}(B^0 \to J/\psi\,\rho^0) = (1.6 \pm 0.6 \pm 0.4) \times 10^{-5}$.

PACS numbers: 13.25.Hw, 12.15.Hh, 11.30.Er

In the Standard Model, the decay $B^0 \to J/\psi\,\rho^0$ can give rise to *CP*-violating asymmetries (directly and through $B^0$-$\overline{B}^0$ mixing). Therefore it is interesting to study the decay mode $B^0 \to J/\psi\,\pi^+\pi^-$ to understand the

$J/\psi\,\rho^0$ component in the final state. Since these decays are Cabibbo and color suppressed, they are a sensitive probe of rare and exotic physics processes, such as penguin contributions and box diagrams containing charged Higgs bosons. These effects may appear as deviations of the branching fraction from the Standard Model prediction of $\mathcal{B}(B^0 \to J/\psi\,\pi^+\pi^-) = (4.6 \pm 0.8) \times 10^{-5}$ [1]. This decay mode has not previously been observed. CLEO quotes an upper limit of $\mathcal{B}(B^0 \to J/\psi\,\rho^0) < 2.5 \times 10^{-4}$ at the 90% confidence level [2]. Here we present the first measurement of $\mathcal{B}(B^0 \to J/\psi\,\pi^+\pi^-)$.

The data used in the present analysis were collected at the PEP-II storage ring with the *BABAR* detector, described in detail elsewhere [3]. Charged particles are detected, and their momenta measured, with a 40-layer drift chamber (DCH) and a five-layer silicon vertex tracker (SVT), both operating in a 1.5 T solenoidal magnetic field. Surrounding the DCH is a detector of internally reflected Cherenkov radiation (DIRC), and outside this is a CsI(Tl) electromagnetic calorimeter (EMC). The iron flux return of the solenoid is instrumented with resistive plate chambers (IFR). The data sample used for the analysis contains approximately 56 million $B\overline{B}$ pairs, corresponding to a luminosity of $51.7\,\mathrm{fb}^{-1}$ recorded near the $\Upsilon(4S)$ resonance. An additional $6.4\,\mathrm{fb}^{-1}$, recorded approximately 40 MeV below the $\Upsilon(4S)$ peak, were used to study continuum backgrounds.

Events containing $B\overline{B}$ pairs are selected based on track multiplicity and event topology [4]. At least three tracks are required to originate near the nominal beam spot, with polar angle in the range $0.41 < \theta_{\rm lab} < 2.54$ rad, transverse momentum greater than $100\,\mathrm{MeV}/c$, and a minimum number of DCH hits used in the track fit. To reduce continuum background the ratio of second to zeroth Fox-Wolfram moment, $R_2 = H_2/H_0$, is required to be less than 0.5. The sum of charged and neutral energy must be greater than 4.5 GeV in the laboratory frame. The primary vertex of the event must be within 0.5 cm of the average measured position of the interaction point in the plane transverse to the beamline.

The $J/\psi$ is reconstructed in the $e^+e^-$ and $\mu^+\mu^-$ final states. Electron candidates must satisfy the requirement that the ratio of calorimeter energy to track momentum lies in the range $0.75 < E/p < 1.3$, the cluster shape and size are consistent with an electromagnetic shower, and the energy loss in the DCH is consistent with that for an electron. If an EMC cluster close to the electron track is consistent with originating from a bremsstrahlung photon, it is combined with the electron candidate.

Muon candidates must satisfy requirements on the number of interaction lengths of IFR iron penetrated ($N_\lambda > 2$), the difference between the measured and expected interaction lengths penetrated ($|N_\lambda - N_\lambda^{\rm exp}| < 2$), the position match between the extrapolated DCH track and the IFR hits, and the average and spread of the number of IFR strips hit per layer.

Pion candidates are accepted if they originate from close to the beam spot and are not consistent with being a kaon. The algorithm uses $\mathrm{d}E/\mathrm{d}x$ information from the SVT and DCH, and the Cherenkov angle and number of photons from the DIRC.

Tracks are required to lie in polar-angle ranges where particle identification efficiency is measured with known control samples. The allowed ranges are $0.41 < \theta_{\rm lab} < 2.41$ rad for electrons, $0.30 < \theta_{\rm lab} < 2.70$ rad for muons, and $0.35 < \theta_{\rm lab} < 2.50$ rad for pions, which correspond approximately to the geometrical acceptances of the EMC, IFR, and DIRC, respectively.

Identified electron and muon pairs are fit to a common vertex and must lie in the $J/\psi$ invariant mass interval 2.95 (3.06) to $3.14\,\mathrm{GeV}/c^2$ for the $e^+e^-$ ($\mu^+\mu^-$) channel.

$B^0$ candidates are formed by combining a $J/\psi$ candidate with a pair of oppositely-charged pion candidates consistent with coming from a common decay point. We also require the positions of the vertices of the lepton pair and the pion pair to be consistent. Further selection requirements are made using two kinematic variables: the difference, $\Delta E$, between the energy of the candidate and the beam energy $E_{\rm beam}^{\rm cm}$ in the center-of-mass frame, and the beam-energy substituted mass, $m_{\rm ES} = \sqrt{(E_{\rm beam}^{\rm cm})^2 - (p_B^{\rm cm})^2}$. After applying the loose requirements $5.2 < m_{\rm ES} < 5.3\,\mathrm{GeV}/c^2$ and $|\Delta E| < 0.12\,\mathrm{GeV}$, approximately one-quarter of events contain more than one $B^0$ candidate, from which we keep the one with the smallest $|\Delta E|$. The distribution of the candidates in $\Delta E$ and $m_{\rm ES}$ is shown in Fig. 1. For the final signal sample, we require $|m_{\rm ES} - 5279.0\,\mathrm{MeV}/c^2| < 9.9\,\mathrm{MeV}/c^2$ and $|\Delta E| < 39\,\mathrm{MeV}$, which correspond to $4\sigma$ and $3\sigma$ ranges in the resolutions for $m_{\rm ES}$ and $\Delta E$. After all selection criteria have been applied, 213 events remain.

An unbinned, extended maximum-likelihood [5] fit is performed on the invariant mass distribution of the two pions for the selected events, to determine the various contributions to the $B^0 \to J/\psi\,\pi^+\pi^-$ events. We consider five categories: (i) $B^0 \to J/\psi\,\rho^0$ events; (ii) $B^0 \to J/\psi\,K_S^0(K_S^0 \to \pi^+\pi^-)$ events; (iii) $B^0 \to J/\psi\,\pi^+\pi^-$ (non-$\rho^0$ signal) events; (iv) background from events without a real $J/\psi$; (v) inclusive-$J/\psi$ background from events containing a real $J/\psi$. A probability density function (PDF) is constructed for each of these five cases. The total PDF is then formed from the sum of the five PDFs and fit to the data. The $B^0 \to J/\psi\,K_S^0$ mode is not considered to be signal for the purposes of determining the branching fraction for $B^0 \to J/\psi\,\pi^+\pi^-$.

The PDF used to model the $B^0 \to J/\psi\,\rho^0$ mode is a relativistic $P$-wave Breit-Wigner function [6]:
$F_\rho(m) = (m\,\Gamma(m)\,P^{2L_{\rm eff}+1})/((m_\rho^2 - m^2)^2 + m_\rho^2\Gamma(m)^2)$,
where $\Gamma(m) = \Gamma_0(\frac{q}{q_0})^3(\frac{m_\rho}{m})(\frac{1+R^2q_0^2}{1+R^2q^2})$. $q(m)$ is the pion momentum in the di-pion rest frame, with $q_0 = q(m_\rho)$. $m \equiv M(\pi^+\pi^-)$ is the two-pion invariant mass and $P$ is the $J/\psi$ momentum in the $B^0$ rest frame. $m_\rho =$

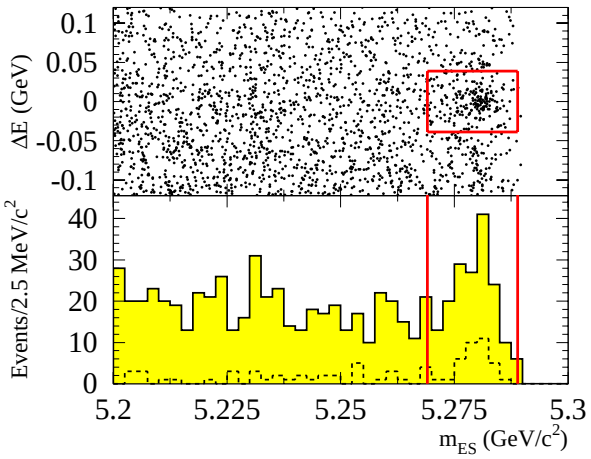


FIG. 1: Signal for $B^0 \to J/\psi\pi^+\pi^-$. The upper plot shows the distribution of events in the $\Delta E$-$m_{\rm ES}$ plane, where the box represents the final selection criteria. The lower plot shows the distribution in $m_{\rm ES}$ of events with $|\Delta E| < 39\,$MeV, where the dashed (solid) line corresponds to events in the $K^0_S$ (non-$K^0_S$) region in $M(\pi^+\pi^-)$ (0.45-0.55 GeV/$c^2$). The vertical lines represent the final selection.

770 MeV/$c^2$, $\Gamma_0 = 150\,$MeV/$c^2$, and $m_\pi = 140\,$MeV/$c^2$. $L_{\rm eff}$ is the effective orbital angular momentum between the $J/\psi$ and the $\rho^0$, which can take any value between 0 and 2 and so is allowed to float in the fit. $R$ is the Blatt-Weisskopf barrier-factor radius [7]. The fit is performed with $R$ equal to two values (0.5 and 1.0 fm) and the results of the two fits are averaged.

The PDF for the $B^0 \to J/\psi K^0_S$ mode is a single Gaussian function with the mass and width fixed to values obtained by fitting a sample of simulated $J/\psi K^0_S$ events. Allowing these parameters to vary in the final $M(\pi^+\pi^-)$ fit does not change the results.

The PDF used to model the $B^0 \to J/\psi\pi^+\pi^-$ (non-$\rho^0$ signal) contains a three-body phase space factor $q(m)P(m)$ and a factor of $P(m)^2$ motivated by angular momentum conservation: $F_{\rm ph}(m) = q(m)P(m)^3$. If the $\pi^+\pi^-$ is in an $S$-wave, angular momentum conservation results in a factor of $P(m)^2$, while a $D$-wave yields the second power of $P(m)$ or higher.

The PDF for the $M(\pi^+\pi^-)$ distribution for background events without a real $J/\psi$ is derived from a fake-$J/\psi$ sample selected in data as described above except that at least one of the lepton candidates must fail the appropriate particle identification requirements. A Monte Carlo study confirms that the $M(\pi^+\pi^-)$ distribution obtained with this procedure correctly describes the shape of the non-$J/\psi$ background. The resulting distribution is parametrized using the sum of two Weibull functions [8] and a Breit-Wigner. The Breit-Wigner describes the $\rho^0$ component of the non-$J/\psi$ background.

The PDF for the $M(\pi^+\pi^-)$ shape for background events containing a real $J/\psi$ is obtained from a simulated $B \to J/\psi X$ sample equivalent to a luminosity of 81 fb$^{-1}$. Events in which the system $X$ is $\pi^+\pi^-$ (non-resonant), $\rho^0$, or $K^0_S$ $(\pi^+\pi^-)$ are removed from the sample. The resulting shape is described by a Weibull function.

The normalization of the background components is obtained from samples in data and simulation. The level of non-$J/\psi$ background is obtained from sidebands of the $J/\psi$ mass distribution in data. The $m_{ES}$ distribution for these sideband candidates is then fit to an ARGUS function [9] to determine how many events pass the final selection criterion. Scaling to the equivalent background in the $J/\psi$ mass region, using an exponential to describe the background shape in the $J/\psi$ mass distribution, the expected non-$J/\psi$ background is found to be 35.7±1.2 events.

The level of inclusive-$J/\psi$ background is obtained from the distribution of $m_{ES}$ for events in the $\Delta E$ signal region in both data and simulation. In each case the $m_{ES}$ distribution is parametrized by a Gaussian function (to represent signal or peaking background) and an ARGUS function. Peaking background originates from $B \to J/\psi X$ decays such as $B \to J/\psi K^*$, $B^+ \to J/\psi\rho^+$, and $B \to J/\psi K_1$, that accumulate near $m_{ES} = 5.279$ GeV/$c^2$.

The non-peaking component of the inclusive-$J/\psi$ background is determined by subtracting the non-$J/\psi$ contribution, on the basis of the scaled sideband events described above, from the total ARGUS background in data. The peaking component is determined from the Gaussian part of the $m_{ES}$ distribution in $B \to J/\psi X$ simulation, where events with $X = \pi^+\pi^-$ (non-resonant), $\rho^0$ and $K^0_S(\pi^+\pi^-)$ have been removed. The sum of peaking and non-peaking components of the inclusive-$J/\psi$ background is found to be 61±11 events, of which the peaking component comprises 6 events. Thus any associated uncertainties, such as branching fractions used in the $J/\psi X$ simulation, will not contribute significantly to the final systematic uncertainty.

The branching fraction is obtained from

$$\mathcal{B}(B^0 \to J/\psi\pi^+\pi^-) = \frac{N_{J/\psi\pi\pi}}{N_{B^0} \times \epsilon_{J/\psi\pi\pi} \times \mathcal{B}(J/\psi \to \ell^+\ell^-)}, \quad (1)$$

where $N_{J/\psi\pi\pi}$ is the total signal yield obtained from the fit, $N_{B^0}$ is the total number of $B^0$ and $\overline{B}^0$ in the data sample [4], and $\epsilon_{J/\psi\pi\pi}$ is the signal efficiency. The $J/\psi$ branching fraction $\mathcal{B}(J/\psi \to \ell^+\ell^-)$ is fixed to 11.81% [10]. We assume that the branching fraction for $\Upsilon(4S) \to B^0\overline{B}^0$ is one-half.

The signal efficiencies for all requirements apart from particle identification criteria are derived from simulation. Lepton and pion identification efficiencies are determined with samples of known muons, electrons and pions in the data from the following processes: $\mu^+\mu^-\gamma$, $\mu^+\mu^-e^+e^-$, $e^+e^-$, $e^+e^-\gamma$, $D^{*+} \to D^0\pi^+$ $(D^0 \to K^-\pi^+)$, and $K^0_S \to \pi^+\,\pi^-$. The efficiencies are determined as a

function of momentum, and polar and azimuthal angle. We find $\epsilon(J/\psi\rho^0) = (27.1 \pm 0.3)\%$ and $\epsilon(J/\psi\pi^+\pi^-$, non-resonant$) = (27.0 \pm 0.3)\%$. The final corrected signal efficiency of $(27.1 \pm 0.2)\%$ is taken as the average of the $J/\psi\rho^0$ and $J/\psi\pi^+\pi^-$ (non-resonant) efficiencies, where the error is from Monte Carlo statistics.

A likelihood fit is performed on the $M(\pi^+\pi^-)$ distribution in data with the normalization of the non-$J/\psi$ background fixed to 35.7 events and the inclusive-$J/\psi$ background to 61. Thus only the yields for $J/\psi\rho^0$, $J/\psi\pi^+\pi^-$ (non-$\rho^0$ signal), and $J/\psi K^0_S$ events are allowed to vary. The results of the fit are overlaid on the data points in Fig. 2. The goodness-of-fit $\chi^2$ is 33.4 for 38 data points.

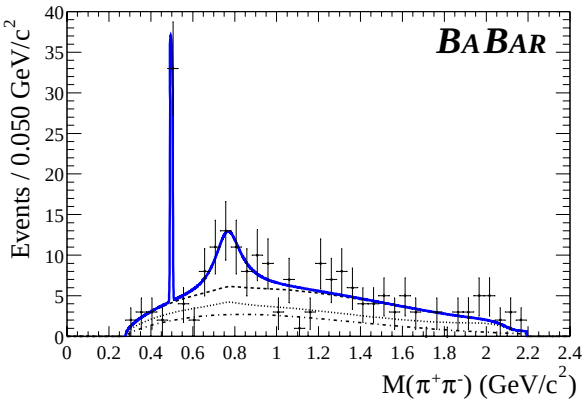


FIG. 2: Distribution of the invariant mass $M(\pi^+\pi^-)$ for events passing all selection criteria. The solid line is the result of the unbinned likelihood fit. The dashed line represents the sum of background and non-$\rho^0$ signal components. The dotted (dot-dashed) line shows the total (inclusive-$J/\psi$) background. The spike corresponds to $B^0 \to J/\psi K^0_S$ events.

The result of the fit is $84 \pm 13$ signal events, of which $28\pm10$ are in the $\rho^0$ component and $55\pm15$ are in the non-$\rho^0$ signal component. The number of events in the $K^0_S$ component is $28\pm5$. Inserting the result into Eq. 1 yields the branching fraction $\mathcal{B}(B^0 \to J/\psi\pi^+\pi^-) = (4.6\pm0.7)\times 10^{-5}$, where the error is statistical.

The signal yield can be checked by counting the number of events passing all the selection criteria and subtracting the estimated numbers of background and $J/\psi K^0_S$ events. This method gives $87 \pm 15$ $J/\psi\pi^+\pi^-$ events, where the error is statistical.

The systematic errors on the final branching fraction measurement arise from uncertainties on the signal efficiency, fitted yield, number of $B\overline{B}$ pairs produced, and $J/\psi \to \ell^+\ell^-$ branching fraction. $N_{B\overline{B}}$ is known to 1.1% with the dominant contribution to the uncertainty coming from the error on the efficiency for the $B^0\overline{B}^0$ selection. $\mathcal{B}(J/\psi \to \ell^+\ell^-)$ is known to 1.7% (fractional) [10].

The uncertainty on the pion identification efficiency is 1.8% per pion. Contributions to this error come from the limited size of the data sample used to determine the efficiency, the uncertainty on the kaon contamination in the sample, and residual differences between the efficiencies for the known pions in data and for pions from $B^0 \to J/\psi\pi^+\pi^-$, determined from Monte Carlo simulation.

Uncertainties on electron and muon particle identification efficiencies come from studies using $B \to J/\psi X$ events in data. Fits to the $M(J/\psi)$ distribution in these events, under different selection criteria, give estimates of the electron and muon identification efficiencies and their errors. The overall error for the identification criteria used in this analysis is 1.3%.

The uncertainty on the determination of the tracking efficiency is 1.3% per track, and is summed for the four tracks from the $B^0$ decay. The efficiency of the convergence requirement on the $\pi^+\pi^-$ vertex fit has been studied with a sample of $\psi(2S) \to \ell^+\ell^-$ decays. Data and simulation are found to be in good agreement, with an associated systematic error of 1%. The unknown $\rho^0$ helicity in the $J/\psi\rho^0$ component of the final sample introduces a systematic error on the efficiency of 2.5%, as determined from the efficiency variation between simulated samples with helicity 0 and 1. The limited amount of simulated data leads to an uncertainty in signal efficiency of 0.7%. To determine the effect of the signal and background shapes and the background yields on the fitted yields, the fixed parameters of these PDFs are varied within their uncertainties, allowing for correlations. This produces a total systematic error due to fit parameter variation of 9.7%, which is dominated by the errors in the background yields. The final fit neglects resonances such as $f_0(980)$, $f_2(1270)$ and $\rho^0(1450)$. Allowing for the addition of such terms in the likelihood function results in a systematic uncertainty on the yield of 2.1%. The total systematic uncertainty from all sources is found to be 12.3%.

The analysis is repeated with variations in the selection criteria. Taking into account statistical correlations between the results, we find that variations are consistent with statistical fluctuations due to the addition or removal of some of the events in the sample.

The branching fraction can be measured separately for events containing a $J/\psi \to e^+e^-$ or a $J/\psi \to \mu^+\mu^-$ candidate. The results from these subsamples are $\mathcal{B}(B^0 \to J/\psi\pi^+\pi^-)_{ee} = (5.3 \pm 1.1) \times 10^{-5}$ and $\mathcal{B}(B^0 \to J/\psi\pi^+\pi^-)_{\mu\mu} = (4.0 \pm 1.0) \times 10^{-5}$, where the errors are statistical.

Another way to model the backgrounds is to use a smoothing algorithm on the simulated $B \to J/\psi X$ and fake-$J/\psi$ data events, rather than impose a parametrization. The resulting PDFs follow fluctuations and check how strongly the fitted signal yields depend on the chosen method of describing the backgrounds. Changing the background modeling in this way alters the total fitted yield by less than one event.

The $M(\pi^+\pi^-)$ distribution shows a clear peak at the

$\rho^0$ mass. The fit result of $28 \pm 10$ events for the $\rho^0$ signal leads to a branching fraction of $\mathcal{B}(B^0 \to J/\psi\,\rho^0) = (1.6 \pm 0.6\,(\mathrm{stat}) \pm 0.4\,(\mathrm{syst})) \times 10^{-5}$. The systematic error includes a contribution from the effect of using an alternative PDF to describe the non-$\rho^0$ signal. The shape is from a polynomial fit to data recorded in $\pi$-$\pi$ scattering experiments [11] and thus provides an empirically-derived shape, in contrast to the default non-$\rho^0$ signal PDF, which is based on a phase-space assumption. The assumption that the non-$\rho^0$ signal is predominantly $S$-wave, and therefore interference with the $\rho^0$ can be neglected, has been checked on data. A significant $S$-wave contribution means that the leptons from the $J/\psi$ have a helicity angle distribution $\propto \sin^2(\theta_{J/\psi})$. For events in data with $M(\pi^+\pi^-) > 1.1\,\mathrm{GeV}/c^2$, we subtract the helicity cosine distribution for events with $m_{ES} < 5.27\,\mathrm{MeV}/c^2$ from the distribution for events in the signal $m_{ES}$ region and find that the shape of the resulting distribution is consistent with $\sin^2(\theta_{J/\psi})$. Interference between $S$- and $P$-wave signal components integrates out in the $M(\pi^+\pi^-)$ projection, as long as the acceptance is symmetric in the cosine of the di-pion helicity angle, $\theta_{\pi\pi}$. Studies using simulated non-resonant $S$-wave events show that there is no significant odd component to the acceptance function in $\cos(\theta_{\pi\pi})$. Consequently, there is no such interference contribution to the $\pi^+\pi^-$ mass distribution

In summary, the branching fraction for $B^0$ meson decay to the final state $J/\psi\pi^+\pi^-$ has been measured for the first time. The result, $\mathcal{B}(B^0 \to J/\psi\pi^+\pi^-) = (4.6 \pm 0.7\,(\mathrm{stat}) \pm 0.6\,(\mathrm{syst})) \times 10^{-5}$, is consistent with the Standard Model prediction [1]. In addition, the technique of fitting the $M(\pi^+\pi^-)$ distribution allows a measurement of the branching fraction for the $J/\psi\,\rho^0$ component. The result is $\mathcal{B}(B^0 \to J/\psi\,\rho^0) = (1.6 \pm 0.6\,(\mathrm{stat}) \pm 0.4\,(\mathrm{syst})) \times 10^{-5}$.

We are grateful for the excellent luminosity and machine conditions provided by our PEP-II colleagues, and for the substantial dedicated effort from the computing organizations that support *BABAR*. The collaborating institutions wish to thank SLAC for its support and kind hospitality. This work is supported by DOE and NSF (USA), NSERC (Canada), IHEP (China), CEA and CNRS-IN2P3 (France), BMBF and DFG (Germany), INFN (Italy), NFR (Norway), MIST (Russia), and PPARC (United Kingdom). Individuals have received support from the A. P. Sloan Foundation, Research Corporation, and Alexander von Humboldt Foundation.

* Also with Università di Perugia, I-06100 Perugia, Italy

[1] The world average values [10] for the branching fractions $B^0 \to J/\psi\,K^{*0}$ and $B^0 \to J/\psi\,K^+\pi^-$ have been scaled by $0.5|V_{cd}|^2/|V_{cs}|^2$ and $|V_{cd}|^2/|V_{cs}|^2$, respectively. The number quoted in the text is the sum of the two scaled values, and assumes that the tree amplitude is dominant.

[2] CLEO Collaboration, M. Bishai *et al.*, Phys. Lett. B **369**, 186 (1996).

[3] BABAR Collaboration, B. Aubert *et al.*, Nucl. Instr. and Meth. **A479**, 1 (2002).

[4] For a description of the $B\overline{B}$ event selection see, for example, Sec. VI of BABAR Collaboration, B. Aubert *et al.*, Phys. Rev. D **65**, 032001 (2002).

[5] R. J. Barlow, Nucl. Instrum. Meth. A **297**, 496 (1990).

[6] J. Pisut and M. Roos, N. Phys. B **6**, 325 (1968).

[7] J. M. Blatt and V. F. Weisskopf, *Theoretical Nuclear Physics* (Wiley, New York, 1952), p. 361.

[8] The Weibull function can be written as $W(m) = C\,V\,(m - M_{\mathrm{on}})^{(C-1)} \times \exp[-V(m - M_{\mathrm{max}})^C]$, where $V = (C-1)/(C(M_{\mathrm{max}} - M_{\mathrm{on}})^C)$. $M_{\mathrm{max}}$ is the position of the function maximum, $M_{\mathrm{on}}$ is the lower kinematic cut-off, and $C$ is a general shape parameter.

[9] ARGUS Collaboration, H. Albrecht *et al.*, Z. Phys. C **48**, 543 (1990).

[10] Particle Data Group Collaboration, D. E. Groom *et al.*, Eur. Phys. J. C **15**, 1 (2000).

[11] M. Gaspero, Nucl. Phys. A **562**, 407 (1993).